An Acetylacetonate-Based Semiconductor−Sensitizer Linkage

Todd A. Heimer, Samuel T. D'Arcangelis, Fereshteh Farzad, Jeremy M. Stipkala, and Gerald J. Meyer*

Department of Chemistry, Johns Hopkins University, Baltimore, Maryland 21218

Received April 17, 1996[⊗]

Coordination compounds of the general type $Ru(dmb)_2(LL)(PF_6)_2$, where dmb is 4,4′-$(CH_3)_2$-2,2′-bipyridine and LL is 4-(CH_3)-4′-(COOH)-2,2′-bipyridine, or 4-(CH_3)-4′-$((CH_2)_3COOH)$-2,2′-bipyridine, or 4-(CH_3)-4′-$((CH_2)_3$-$COCH_2COOC_2H_5)$-2,2′-bipyridine were prepared for the attachment to semiconductor metal oxide surfaces. The optical and redox properties of these compounds in dichloromethane solution are reported. Binding to porous nanostructured TiO_2 films was analyzed with the Langmuir adsorption isotherm model. Photoelectrochemical measurements of the modified TiO_2 electrodes in regenerative solar cells are reported. The results indicate that intimate electronic coupling between the surface link and the chromophoric ligand is not a strict requirement in the design of sensitizers for photovoltaic applications. Interfacial kinetics for recombination of the electron in the solid with the oxidized form of the sensitizer were quantitated by excited state absorption spectroscopy.

The covalent attachment of well-defined compounds to solid surfaces is an important step in the development of molecular-level devices.[1] At metal oxide interfaces, this chemistry has utilized linkages based on silanes,[2] amides,[3] ethers,[4] esters,[5] and phosphonates.[6] Renewed interests in modified semiconductor surfaces have focused on the sensitization of porous nanostructured metal oxide films to visible light. Regenerative solar cells based on these materials have recently experienced an order of magnitude increase in sunlight-to-electricity conversion efficiency, and practical applications appear likely.[7] The most efficient cells are based on Ru(II) polypyridyl compounds with carboxylic acid groups bound to nanocrystalline TiO_2. The reaction of carboxylic acid functionalities with surface hydroxyl groups was initially proposed to form covalent ester bonds,[5] and there now exist some vibrational data which support this assignment.[8,9] Sensitizers bound to metal oxide surfaces through this linkage display high stability in most anhydrous organic solvents and in acidic aqueous solution. However, in neutral and basic aqueous solutions the sensitizers are rapidly removed from the surface.

A chemical bond between a sensitizer and a semiconductor surface not only serves to anchor the sensitizer in place but also may enhance electronic coupling and/or alter surface state energetics. Therefore, an important objective in the next generation of solar cells is to develop new molecular surface linkages. When considering strategies for binding Ru(II) polypyridyl sensitizers to TiO_2 materials we were attracted to acetylacetonate (acac) and its derivatives. Acac, β-ketoesters, and related β-diketones are known to form strong chelate rings with transition metal ions.[10] Of relevance to TiO_2 materials, Ti(IV) coordination compounds that contain acac and alkoxides are well-known. In some cases, the acac ligand is stable toward hydrolysis reactions over a wide pH range.[11] Acac also forms adducts with Ti(III) compounds[12] and is therefore an excellent candidate for optoelectronic applications based on TiO_2 materials.

In this manuscript we report the preparation, spectroscopic, surface attachment, and photoelectrochemical properties of a Ru(II) compound which contains a 2,2′-bipyridine with a pendant acac derivative (abbreviated bpy-acac). Ru(II) compounds with bpy−carboxylic acid groups (abbreviated bpy-

[⊗] Abstract published in *Advance ACS Abstracts,* August 15, 1996.

(1) Swalen, J. D.; Allara, D. L.; Andrade, J. D.; Chandross, E. A.; Garoff, S.; Israelachvili, J.; McCarthy, T. J.; Murray, R.; Pease, R. F.; Rabolt, J. F.; Wynee, K. J.; Yu, H. *Langmuir* **1987**, *3*, 932.

(2) (a) Moses, P. R.; Wier, L.; Murray, R. W. *Anal. Chem.* **1975**, *47*, 1883. (b) Haller, I. *J. Am. Chem. Soc.* **1978**, *100*, 8050. (c) Ghosh, P.; Spiro, T. G. *J. Am. Chem. Soc.* **1980**, *102*, 5543. (d) Bookbinder, D. C.; Wrighton, M. S. *J. Electrochem. Soc.* **1983**, *130*, 1080. (e) Miller, C. J.; Widrig, C. A.; Charych, D. H.; Majda, M. *J. Phys. Chem.* **1988**, *92*, 1928. (f) Ford, W. E.; Rodgers, M. A. J. *J. Phys. Chem.* **1994**, *98*, 3822.

(3) (a) Moses, P. R.; Murray, R. W. *J. Electroanal. Chem.* **1977**, *77*, 393. (b) Shepard, V. R.; Armstrong, N. R. *J. Phys. Chem.* **1979**, *83*, 1268. (c) Fox, M. A.; Nabs, F. J.; Voynick, T. A. *J. Am. Chem. Soc.* **1980**, *102*, 4036.

(4) Zou, C.; Wrighton, M. S. *J. Am. Chem. Soc.* **1990**, *112*, 7578.

(5) (a) Fujihara, M.; Ohishi, N.; Osa, T. *Nature* **1977**, *268*, 226. (b) Anderson, S.; Constable, E. C.; Dare-Edwards, M. P.; Goodenough, J. B.; Hamnett, A.; Seddon, K. R.; Wright, R. D. *Nature* **1979**, *280*, 571. (c) Dare-Edwards, M. P.; Goodenough, J. B.; Hamnett, A.; Seddon, K. R.; Wright, R. D. *Faraday Discuss. Chem. Soc.* **1980**, *70*, 285. (d) Fox, M. A.; Nobs, F. J.; Voynick, T. A. *J. Am. Chem. Soc.* **1980**, *102*, 4029. (e) Dabestani, R.; Bard, A. J.; Campion, A.; Fox, M. A.; Mallouk, T. E.; Webber, S. E.; White, J. M. *J. Phys. Chem.* **1988**, *92*, 1872.

(6) Pechy, P.; Rotzinger, F. P.; Nazeeruddin, M. K.; Kohle, O.; Zakeeruddin, S. M.; Humphry-Baker, R.; Gratzel, M. *J. Chem. Soc., Chem Commun.* **1995**, 65.

(7) (a) Desilvestro, J.; Gratzel, M.; Kavan, L.; Moser, J.; Augustynski, J. *J. Am. Chem. Soc.* **1985**, *107*, 2988. (b) Nazeeruddin, M. K.; Liska, P.; Moser, J.; Vlachopoulos, N.; Gratzel, M. *Helv. Chim. Acta* **1990**, *73*, 1788. (c) O'Regan, B.; Gratzel, M. *Nature* **1991**, *353*, 737. (d) Nazeeruddin, M. K.; Kay, A.; Rodicio, I.; Humphry-Baker, R.; Muller, E.; Liska, P.; Vlachopoulos, N.; Gratzel, M. *J. Am. Chem. Soc.* **1993**, *115*, 6382.

(8) (a) Heimer, T. A.; Bignozzi, C. A.; Meyer, G. J. *J. Phys. Chem.* **1993**, *97*, 11987. (b) Argazzi, R.; Bignozzi, C. A.; Heimer, T. A.; Castellano, F. N.; Meyer, G. J. *Inorg. Chem.* **1994**, *33*, 5741.

(9) (a) Meyer, T. J.; Meyer, G. J.; Pfenning, B.; Schoonover, J. R.; Timpson, C.; Wall, J. F.; Kobusch, C.; Chen, X.; Peek, B. M.; Wall, C. G.; Ou, W.; Erickson, B. W.; Bignozzi, C. A. *Inorg. Chem.* **1994**, *33*, 3952. (b) Heimer, T. A.; Meyer, G. J. *Proc.-Electrochem. Soc.* **1995**, *121*, 141.

(10) Fackler, J. P. *Prog. Inorg. Chem.* **1966**, *7*, 361, and references therein.

(11) (a) Sanchez, C.; Babonneau, F.; Doeuff, S.; Leaustic, A. in *Ultrastructure Processing of Advanced Ceramics*; Mackenzie, J. D., Ulrich, D. R. Eds.; Wiley: New York, 1988; p 77. (b) Babonneau, F.; Leaustic, A.; Livage, J. In *Better Ceramics Through Chemistry III*; Brinker, C. J., Clark, D. E., Ulrich, D. R., Eds.; Materials Research Society Symposium Proceedings 121; Materials Research Society: New York, 199X; p 317.

(12) (a) Figgis, B. N.; Lewis, J.; Mabbs, F. *J. Chem. Soc.* **1963**, 2473. (b) Cox, M.; Lewis, J.; Nyholm, R. S. *J. Chem. Soc.* **1965**, 2840. (c) McGarvey, B. R. *J. Chem. Phys.* **1963**, *38*, 388. (d) Thewalt, U.; Adam, I. Z. *Naturforsch., B* **1978**, *33*, 142.

S0020-1669(96)00419-3 CCC: $12.00

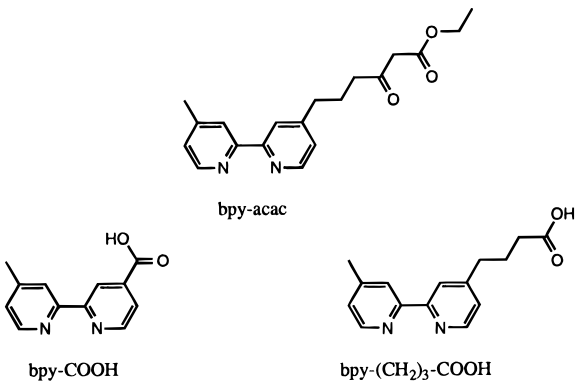

COOH and bpy-$(CH_2)_3$COOH) were prepared to explore the possible benefits of the acac linkage. The compounds synthesized allow two different comparisons to be made. The first is between two ruthenium compounds containing one carboxylic acid group. One compound has the carboxylic acid bound directly to the bipyridine ring (4-CH_3-4′-COOH,-2,2′-bipyridine, abbreviated bpy-COOH) while the other has a *n*-propyl spacer between the bipyridine ring and the carboxylic acid group (4-CH_3-4′-$(CH_2)_3$-COOH,-2,2′-bipyridine, abbreviated bpy-$(CH_2)_3$-COOH). The second comparison is between linkers of equal length, but with different anchors, one carboxylic acid and one acetylacetonate. An important finding from these studies is that intimate electronic communication between the surface binding group and the chromophoric ligand is not a strict requirement in the design of efficient sensitizers for photovoltaic applications.

Experimental Section

Materials. All reagents purchased were used without further purification. Solvents were HPLC grade and were used without further purification, except THF, which was distilled from sodium benzophenone ketyl. Syntheses were performed under inert atmosphere. Column chromatography was performed with 230−400 mesh silica. Both chromatography and extractions were monitored with Analtech Uniplate silica gel GHLF prepared TLC plates.

Ligand and Ruthenium Precursor Preparations. 4′-Methyl-4-carboxy-2,2′-bipyridine (bpy-COOH) was prepared in the manner described by Strouse et al. as a byproduct in the synthesis of 4′-methyl-4-formyl-2,2′-bipyridine.[13]

4-(3-Formylpropyl)-4′-methyl-2,2′-bipyridine was prepared with the following modification of the synthesis developed by Della Ciana et al.:[14] 5.17 mL of a 2.5-M hexane solution (12.9 mmol) of *n*-butyllithium was added to 1.81 mL (12.9 mmol) of diisopropylamine in 10 mL of anhydrous THF. This solution was added dropwise to 2.5 g (13.6 mmol) of 4,4′-dimethyl-2,2′-bipyridyl suspended in 50 mL of anhydrous THF at −78 °C. After an hour of stirring, 1.60 mL (13.6 mmol) of 2-(2-bromoethyl)-1,3-dioxolane was added at once, and the mixture was allowed to warm to room temperature overnight. The reaction was quenched with 20 mL of saturated aqueous NaCl. The organic layer was separated and combined with CH_2Cl_2 extractions (3 × 20 mL) from the aqueous layer. The solvent was removed and the residue was dissolved in 75 mL 1.0 M HCl and was warmed to 60 °C for 3 h. The cooled solution was neutralized with saturated aqueous Na_2CO_3 and was extracted with CH_2Cl_2 (3 × 20 mL). The CH_2Cl_2 solution was dried over $MgSO_4$, and the solution was loaded onto a CH_2Cl_2/silica column. 4-(3-Formylpropyl)-4′-methyl-2,2′-bipyridine eluted second during chromatography with a CH_2Cl_2/Et_2O solution gradient. The gradient was formed by increasing the percent volume of Et_2O by 5−10% for each column length eluted. This procedure produced 1.5 g (6.2 mmol), 45% yield. NMR spectra are in agreement with literature data.[14]

***cis*-Bis(4,4′-dimethyl-2,2′-bipyridine)ruthenium dichloride dihydrate [$(dmb)_2RuCl_2\cdot 2H_2O$],** was prepared as described by Sullivan et al.[15] Tris(bipyridyl) ruthenium complexes were prepared as described by Sullivan et al.[15]

General Procedure for Purification of Tris(bipyridyl)ruthenium Complexes. Crude residues containing the desired ruthenium species were dissolved in MeOH or EtOH/H_2O and were loaded directly onto a silica column, packed with MeOH. All non-ionic substances were quickly eluted with MeOH. Elution of some ruthenium(II) species functionalized with nonpolar groups proceeded next. When the eluent was clear, elution of polar-functionalized Ru (II) species proceeded with MeOH saturated with NaCl. The fractions containing the desired functionalized Ru (II) species were combined, and the MeOH was removed. The residue was dissolved in water and poured into a separatory funnel containing CH_2Cl_2. Enough $NaPF_6$ was added to the funnel such that the ruthenium species resided largely in the CH_2Cl_2 layer. The aqueous layer was then extracted with CH_2Cl_2 (3× or 4×), and the combined extractions were dried over $MgSO_4$ and gravity filtered. Removal of the solvent produced the product, which was purified further by the following recrystallization technique: The crude product was diluted in a minimum of CH_2Cl_2 in a glass container large enough to contain triple the volume of solution. This open container was placed inside a larger container. Enough Et_2O was added to the larger container to come to half the height of the smaller container. The larger container was capped, and the solvents were allowed to diffuse into each other, undisturbed, for a day or two. The resulting precipitate was separated from solution by decanting or filtration and dried under vacuum.

[Bis(4,4′-dimethyl-2,2′-bipyridyl)][4-(3-carboxypropyl)-4′-methyl-2,2′-bipyridyl]ruthenium Bis(hexafluorophosphate) (Abbreviated $Ru(dmb)_2(bpy\text{-}(CH_2)_3COOH)^{2+}$). The following modified reaction employs a permanganate oxidation similar to that found in Della Ciana et al.[14] A 65.8 mg (0.417 mmol) sample of $KMnO_4$ was dissolved in 8 mL of acetone and was added dropwise to a 50 mL round-bottom flask containing 100 mg (0.417 mmol) of 4′-(formylpropyl)-4-methyl-2,2′-bipyridine in 2 mL of acetone, until the permanganate color persisted for more than 1 min. Then 20% more $KMnO_4$ solution was added, and the mixture was allowed to stir overnight. The reaction was quenched with a few drops of concentrated aqueous formaldehyde. The solution was filtered to remove the manganese byproducts, and the solvent was removed. The residue was introduced to 25 mL of a 50/50 solution of EtOH/H_2O and 168 mg (0.333 mmol) of ruthenium bis(dimethylbipyridyl) dichloride dihydrate. The mixture was refluxed for 1 h, allowed to cool, and loaded directly onto a MeOH/silica column. The general procedure for purification of tris(bipyridyl)ruthenium complexes was employed, producing 125 mg (0.123 mmol), 37% overall yield (based on $(dmb)_2RuCl_2\cdot 2H_2O$). ^{1}H NMR: δ 8.19−8.14 (6 H, m), 7.47−7.39 (6 H, m), 7.18−7.13 (6 H, m), 2.81 (2 H, t, J = 7.8 Hz), 2.5 (3 H, s), 2.5 (3 H, s), 2.5 (3 H, s), 2.5 (3 H, s), 2.5 (3 H, s), 2.38 (2 H, t, J = 7.2 Hz), 1.95 (2 H, tt, J = 7.8 Hz, J = 7.2 Hz). FAB MS: m/z = 871 ($[M - PF_6^-]^+$), 725 ($[M - 2PF_6^- - H^+]^+$), 469 ($[M - 2PF_6^- - LL - e^-]^+$), 363 ($[M - 2PF_6^-]^{2+}$). Anal. Calcd: C, 46.12; H, 3.97; N, 8.27. Found: C, 44.24; H, 3.76; N, 7.80.

Bis(4,4′-dimethyl-2,2′-bipyridyl)(4′-methyl-4-carboxy-2,2′-bipyridine)ruthenium Bis(hexafluorophosphate) (Abbreviated $Ru(dmb)_2(bpy\text{-}COOH)^{2+}$). An 80 mg (0.38 mmol) sample of 4′-methyl-4-carboxy-2,2′-bipyridine was refluxed with 131 mg (0.25 mmol) $(dmb)_2RuCl_2\cdot 2H_2O$, in 25 mL of a 50/50 EtOH/H_2O solution, for 3 h under argon. The solution was cooled and was loaded directly onto a MeOH/silica column. The general procedure for purification of tris(bipyridyl)ruthenium complexes was employed, producing 100 mg (0.10 mmol), 41% yield (based on $(dmb)_2RuCl_2\cdot 2H_2O$). ^{1}H NMR: δ 10.11 (1 H s), 8.81 (1 H, s), 8.43 (1 H, s), 8.23 (4 H, m), 7.93 (1 H, d, J = 5.7 Hz), 7.69 (1 H, d, J = 4.4 Hz), 7.49−7.39 (5 H, m), 7.23−7.14 (5 H, m), 2.5 (3 H, s), 2.5 (3 H, s), 2.5 (3 H, s), 2.5 (3 H, s), 2.5 (3 H, s), 2.5 (3 H, s). FAB MS: m/z = 829 ($[M - PF_6^-]^+$), 684 ($[M - 2PF_6^- + e^-]^+$), 469 ($[M - 2PF_6^- - LL - e^-]^+$), 342 ($[M - 2PF_6^-]^{2+}$). Anal. Calcd: C, 44.41; H, 3.52; N, 8.63. Found: C, 44.75; H, 3.37; N, 8.46.

Bis(4,4′-dimethyl-2,2′-bipyridyl)(4-(formylpropyl)-4′-methyl-2,2′-bipyridyl)ruthenium Bis(hexafluorophosphate). A 360 mg (1.5

(13) Strouse, G. F.; Schoonover, J. R.; Duesing, R.; Boyde, S.; Jones, W. E., Jr.; Meyer, T. J. *Inorg. Chem.* **1995**, *34*, 473.
(14) Della Ciana, L.; Hamachi, I.; Meyer, T. J. *J. Org. Chem.* **1989**, *54*, 1731.
(15) Sullivan, B. P.; Salmon, D. J.; Meyer, T. J. *Inorg. Chem.* **1978**, *17*, 3334.

mmol) sample of 4′-(formylpropyl)-4-methyl-2,2′-bipyridine was refluxed with 520 mg (1.0 mmol) of $(dmb)_2RuCl_2 \cdot 2H_2O$, in 100 mL of a 50/50 EtOH/H_2O solution, for 3 h under argon. The solution was cooled, and was loaded directly onto a MeOH/silica column. The general procedure for purification of tris(bipyridyl) ruthenium complexes was employed, producing 250 mg (0.10 mmol), 25% yield (based on $(dmb)_2RuCl_2 \cdot 2H_2O$). ^{1}H NMR: δ 8.19−8.15 (6 H, m), 7.46−7.40 (6 H, m), 7.14−7.12 (6 H, m), 2.76 (2 H, t, $J = 7.2$ Hz), 2.48 (2 H, m) 2.5 (3 H, s), 2.5 (3 H, s), 2.5 (3 H, s), 2.5 (3 H, s), 2.5 (3 H, s) , 1.92 (2 H, tt, $J = 7.2$ Hz, $J \sim 7.2$ Hz). Anal. Calcd: C, 46.85; H, 4.03; N, 8.41. Found: C, 46.93; H, 4.14; N, 8.02.

Bis(4,4′-dimethyl-2,2′-bipyridyl)[4-[4-oxo-5-(ethoxycarbonyl)pentyl]-4′-methyl-2,2′-bipyridyl]ruthenium Bis(hexafluorophosphate) (Abbreviated $Ru(dmb)_2(bpy\text{-}acac)^{2+}$). The following preparation is based on the modified version of the Lewis acid-catalyzed keto ester synthesis described by Holmquist and Roskamp.[16] A 215 mg (0.215 mmol) sample of bis-(4,4′-dimethyl-2,2′-bipyridyl)][4-(formylpropyl)-4′-methyl-2,2′-bipyridyl]ruthenium bis(hexafluorophosphate), was dissolved in 8 mL of CH_2Cl_2, and was added dropwise over a period of 10 min to a suspension of 215 μL (2.15 mmol) of ethyl diazoacetate, $NNHCCOOCH_2CH_3$, and 41 mg (0.215 mmol) of anhydrous $SnCl_2$. Evolution of nitrogen was observed early in the addition step. After overnight reaction, the CH_2Cl_2 was removed, and the residue was dissolved in methanol containing a small amount of water and acetone to complete solution. The general procedure for purification of tris-(bipyridyl)ruthenium complexes was employed, producing 92 mg (0.085 mmol), 39% yield. ^{1}H NMR: δ 8.19−8.14 (6 H, m), 7.47−7.41 (6 H, m), 7.15−7.13 (6 H, m), 4.07 (2 H, q, $J = 7.2$ Hz), 3.37 (1 H, s), 2.75 (2 H, t, $J = 8.4$ Hz), 2.61 (2 H, t, $J = 6.9$ Hz), 2.5 (3 H, s), 2.5 (3 H, s), 2.5 (3 H, s), 2.5 (3 H, s), 2.5 (3 H, s), 1.90 (2 H, tt, $J = 8.4$ Hz, $J = 6.9$ Hz), 1.18 (3 H, t, $J = 6.9$ Hz). FAB MS: $m/z = 941$ ($[M - PF_6^-]^+$), 795 ($[M - 2PF_6^- + e^-]^+$), 469 ($[M - 2PF_6^- - LL - e^-]^+$), 398 ($[M - 2PF_6^-]^{2+}$). Anal. Calcd: C, 47.56; H, 4.27; N, 7.74. Found: C, 47.62; H, 4.21; N, 7.55.

TiO_2 and ZrO_2 Preparation. Transparent TiO_2 films were prepared from TiO_2 colloidal solutions in a manner analogous to that previously described.[17] A 50 mL aliquot of $Ti(i\text{-}OPr)_4$ (Gelest) (or 76 mL of 70% $Zr(i\text{-}OPr)_4$ in 2-propanol (Aldrich)) was added over 10 min via an addition funnel to a stirred solution of 300 mL of deionized water and 2.1 mL of 70% nitric acid in a three-neck 500 mL round-bottom flask. The other necks were left open to air. A flaky white precipitate formed immediately upon addition of the alkoxide. The mixture was then heated to reflux with continued stirring for 8 h. During this time the precipitate dissolved and the solution became nearly transparent. The solution was then cooled and the final volume was adjusted with water to achieve a concentration of 150 −170 g of MO_2 per liter (based on complete reaction of the initial $M(i\text{-}OPr)_4$).

Approximately 25 mL of the 150 g/L MO_2 solution was placed in a 50 mL round-bottom flask with a 14/20 ground glass joint. The ground glass stopper was installed, turned one quarter turn to lock it in place, and wired shut with copper wire. The flask was then placed in an enclosed oven and heated at 200 °C overnight. At this temperature the pressure in the flask approaches 2 atm. After being cooled to room temperature the mixture had the consistency and appearance of white glue. A 1.5 g sample of Carbowax 2000 (Aldrich) was added and the mixture stirred for an additional 6−8 h. Thin film electrodes are prepared by depositing a few milliliters of this mixture onto conductive glass and spreading the material with a glass test tube. Sintering is then performed in air at 450 °C for 30 min. The electrodes were then cooled to room temperature and either used immediately for surface attachment or stored in ethanol for future use.

Surface Attachment Chemistry. The sensitizers were anchored to TiO_2 or ZrO_2 surfaces by soaking in ∼5 mM dichloromethane solutions for 24 h or longer followed by rinsing in dichloromethane. For adsorption isotherms, the electrodes were placed in sensitizer solutions of known concentration for 24 h. The amount of dye on the surface was determined spectroscopically.

Spectroscopic Measurements. NMR. ^{1}H NMR was obtained on a Bruker 300AMX FT-NMR spectrometer.

Absorbance. UV−vis absorbance measurements were made on a Hewlett-Packard 8451A diode array spectrophotometer. Time-resolved absorbance measurements were made on the apparatus described previously.[8b] Samples were excited with ∼10 mJ/pulse of 532 nm light (8 ns fwhm) and the instrument response function is ∼20 ns. At this wavelength <5 mJ/pulse are absorbed by the surface attached dye.

Photoluminescence. Corrected photoluminescence (PL) spectra were obtained with a Spex Fluorolog which had been calibrated with a standard NBS tungsten−halogen lamp. PL quantum yields were made with $Ru(bpy)_3(PF_6)_2$ as a quantum counter, and lifetimes were obtained with an apparatus which has been previously described.[18]

Electrochemistry. Electrochemistry was performed in 0.1 M tetrabutylammonium hexafluorophosphate (Aldrich, TBAH) dichloromethane electrolyte. The TBAH was recrystallized from ethanol and the dichloromethane was refluxed over CaH under argon until immediately before use. A BAS Model CV27 potentiostat was used in a standard three-cell arrangement consisting of a Pt working electrode, a Pt gauze counterelectrode, and a $Ag/AgNO_3$ reference electrode. Approximately millimolar concentrations of the compounds were dissolved in the electrolyte. The electrochemical measurements were performed in a Vacuum Atmospheres nitrogen-filled drybox.

Cyclic voltammetry of the sensitizers bound to TiO_2 was performed in a similar manner with a modified TiO_2 electrode as working electrode.

Photoelectrochemistry. Photoelectrochemical measurements were performed in a two-electrode sandwich cell arrangement as previously described.[9b] Briefly, ∼10 μL of electrolyte was sandwiched between a TiO_2 electrode and a Pt-coated tin oxide electrode. The TiO_2 was illuminated with a 450 W Xe lamp coupled to either a *f*/0.22 m monochromator for IPCE measurements or a 385 nm cut-off filter for I_{sc} and V_{oc} measurements under "white" light illumination. Photocurrents and voltages were measured with a Keithly Model 617 digital electrometer. Incident irradiances were measured with a calibrated silicon photodiode from UDT Technologies and a Molectron power meter. Irradiance under "white" light conditions was 330 mW/cm^2. The supporting electrolyte was 0.5 M NaI/0.05 M I_2 in propylene carbonate.

Photocurrent stability tests were performed in a sandwich cell arrangement. The supporting electrolyte was 0.5 M NaI/0.05 M I_2 in propylene carbonate. An inert spacer was placed between the working and counter electrode to minimize solvent evaporation. The samples were excited with 1.2 mW/cm^2 of 460 ± 20 nm light for times up to 15 h. The photocurrent was collected on a Keithly Model 617 digital electrometer and was transferred to a 486 microprocessor through a GPIB bus with code written in HP Basic.

Fast Atom Bombardment Mass Spectroscopy. FAB MS was obtained on a VG-Analytical Model 80 mass spectrometer. FAB MS samples were suspended in a *p*-nitrobenzyl alcohol matrix. Observed isotopic distribution of ruthenium bipyridyl complexes are consistent with calculated distributions. Dicationic ruthenium species exhibit compressed isotopic distribution. Elemental analyses were performed at Desert Analytics.

Results

The preparation of ruthenium polypyridyl compounds containing an acac derivative or carboxylates was accomplished in high yield. For the acac compounds, it was found that coupling the bipyridyl-containing aldehyde to diazoacetate was best performed with the ligand already coordinated to the Ru(II) metal center. 4,4′-$(CH_3)_2$-2,2′-bipyridine (dmb) ligands were utilized to help ensure that the MLCT excited state would possess an electron localized on the surface-bound ligand for all the sensitizers.

The absorption spectra of the sensitizers in dichloromethane are shown in Figure 1. The $\pi-\pi^*$ transitions of the ligand are observed in the UV region and the broad visible absorbances are metal-to-ligand charge-transfer (MLCT) bands. Visible excitation into the MLCT bands leads to room temperature

(16) Holmquist, C. R.; Roskamp, E. J. *J. Org. Chem.* **1989**, *54*, 3258.
(17) O'Regan, B.; Moser, J.; Anderson, M.; Gratzel, M. *J. Phys. Chem.* **1990**, *94*, 8720.
(18) Castellano, P. C.; Heimer, T. A.; Thandasetti, M.; Meyer, G. J. *Chem. Mater.* **1994**, *6*, 1041.

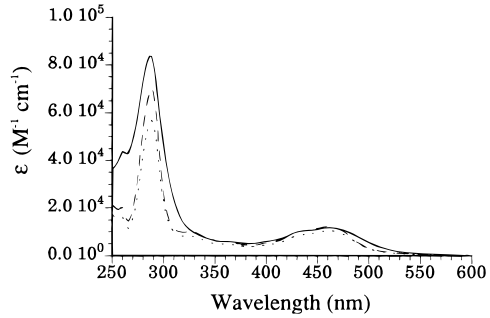

Figure 1. Absorption spectra of the three sensitizers in dichloromethane: (—) $Ru(dmb)_2(bpy\text{-}COOH)(PF_6)_2$; (- -) $Ru(dmb)_2(bpy\text{-}(CH_2)_3COOH)(PF_6)_2$; (— — —) $Ru(dmb)_2(bpy\text{-}acac)(PF_6)_2$. The instrument resolution is ±2 nm.

Table 1. Optical Properties of the Sensitizers in Dichloromethane

sensitizer	λ_{abs}[a] (nm)	ϵ[b] (M^{-1} cm^{-1})	λ_{PL}[c] (nm)	φ[d]	τ[e] (ns)
$Ru(dmb)_2(bpy\text{-}COOH)(PF_6)_2$	462	11 700	650	0.084	920
$Ru(dmb)_2(bpy\text{-}(CH_2)_3COOH)(PF_6)_2$	462	10 400	625	0.104	830
$Ru(dmb)_2(bpy\text{-}acac)(PF_6)_2$	462	12 200	620	0.103	840

[a] The visible absorption maximum, ±2 nm. [b] The molar extinction coefficient at the visible absorption maximum. [c] The corrected PL maximum, ±4 nm. [d] The PL quantum yield. [e] The excited state lifetime, ±10 ns.

Table 2. Electrochemical Properties of the Sensitizers in Dichloromethane Electrolyte

sensitizer	$E_{1/2}(Ru^{III/II})$ V: Pt[a]	$E_{1/2}(Ru^{III/II})$ V: TiO_2[b]	Γ[c] (mol/cm^2)
$Ru(dmb)_2(bpy\text{-}COOH)(PF_6)_2$	0.99	0.90	$8 \pm 2 \times 10^{-9}$
$Ru(dmb)_2(bpy\text{-}(CH_2)_3COOH)(PF6)_2$	0.93	0.87	$3 \pm 2 \times 10^{-9}$
$Ru(dmb)_2(bpy\text{-}acac)(PF_6)_2$	0.92	0.90	$2 \pm 2 \times 10^{-9}$

[a] Half-wave potential assigned to the $Ru^{III/II}$ couple for the sensitizers measured at a Pt working electrode in 0.1 M TBAH electrolyte vs a $Ag/Ag(NO_3)$ reference. [b] Half-wave potential for the sensitizers bound to nanocrystalline TiO_2 films as described in the Experimental Section. [c] The electroactive surface coverage measured by integration of the anodic or cathodic waves obtained at 0.5 mV/s. The error represents one standard deviation for three representative samples.

photoluminescence (PL) in argon saturated dichloromethane. Excitation spectra agree well with the absorption spectra indicating that the PL is from the sensitizers. Time-resolved PL decays are well fit to a single exponential model. Spectroscopic data are summarized in Table 1.

The electrochemical properties of the sensitizers were explored by cyclic voltammetry in dichloromethane electrolyte. The sensitizers were reversibly oxidized at positive potentials, and the redox chemistry is assigned to the $Ru^{III/II}$ couple. The $Ag/Ag(NO_3)$ reference used was found to be ~350 mV vs SSCE in 0.1 M TBAH acetonitrile using ferrocene as an internal standard. The sensitizers bound to TiO_2 electrodes also display stable voltammograms. The measured $E_{1/2}$ for the $Ru^{III/II}$ couple are close to those measured at Pt in free solution, Table 2. The peak anodic and cathodic currents are approximately equal within experimental error. The voltammograms shown in Figure 2 are not affected by stirring the solution. At slower scan rates (0.5−1 mV/s) the waves continue to broaden and the observed current is larger than that predicted by extrapolation of the data shown in the figure. Integration of the anodic and cathodic waves at 0.5 mV/s provides an estimate of the electro-active surface coverage which are summarized in Table 2.

Surface binding was monitored spectroscopically by measuring the change in attenuance of the film after soaking an electrode for 12 h in sensitizer dichloromethane solutions of

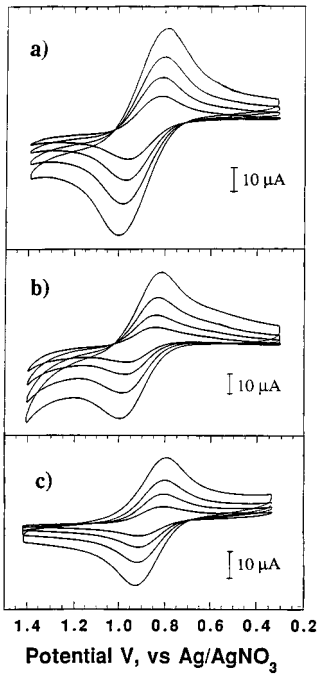

Figure 2. Cyclic voltammograms for the senitizers bound to nanocrystalline TiO_2 films in 0.1 M TBAH in CH_2Cl_2: (a) $Ru(dmb)_2(bpy\text{-}COOH)(PF_6)_2$; (b) $Ru(dmb)_2(bpy\text{-}acac)(PF_6)_2$; (c) $Ru(dmb)_2(bpy\text{-}(CH_2)_3\text{-}COOH)(PF_6)_2$. The data were recorded at 200, 100, 50, and 20 mV/s.

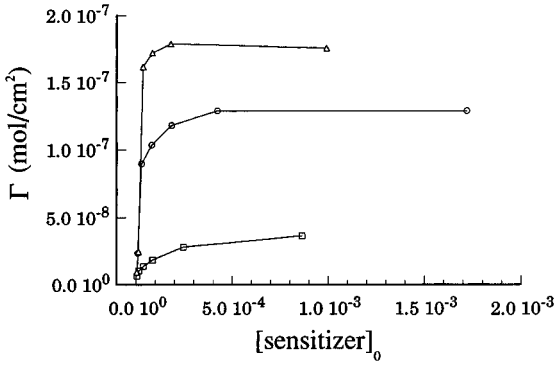

Figure 3. Adsorption isotherms for the three sensitizer bound to TiO_2 in dichloromethane solution. The circles correspond to $Ru(dmb)_2(bpy\text{-}(CH_2)_3COOH)(PF_6)_2$, squares to $Ru(dmb)_2(bpy\text{-}acac)(PF_6)_2$, and triangles to $Ru(dmb)_2(bpy\text{-}COOH)(PF_6)_2$.

varying concentration. The results of such a study are shown in Figure 3. The surface coverage reaches a limiting value at high solution concentrations for all sensitizers. Analysis based on the Langmuir adsorption isotherm model[6,7b,9] yields estimates of the surface adduct formation constants which are summarized in Table 3. The higher adduct formation constant for $Ru(dmb)_2(bpy\text{-}COOH)^{2+}$ when compared to $Ru(dmb)_2(bpy\text{-}(CH_2)_3\text{-}COOH)^{2+}$ is consistent with the expected increased acidity due to inductive effects from the bipyridine ring.

Figure 4 shows the incident photon-to-current efficiency (IPCE) vs excitation wavelength for the three TiO_2 bound sensitizers with a 0.5 M NaI/0.05 M I_2 propylene carbonate electrolyte. Under these conditions the IPCE without a sensitizer is <1% in the visible region. The photoelectrochemical properties were also explored with white light excitation in a two electrode sandwich cell arrangement. The photoelectrochemical data are summarized in Table 3. The long term stability of the observed photocurrent was explored with 1.2 mW/cm^2 of 460 nm light excitation. It was found that the observed photocurrent gradually decreased with time for all three sensitizers. On the basis of the average photocurrent for three samples of each sensitizer, the amount of time required for the

Table 3. Photoelectrochemical Properties of Sensitizers Anchored to TiO_2

sensitizer	I_{sc}[a] (mA/cm^2)	V_{oc}[a] (mV)	V_{oc}[b] (mV)	IPCE$_{max}$[c]	$\Gamma \times 10^{8}$[d] (mol/cm^2)	K_{ad}[e] (M^{-1})
$Ru(dmb)_2(bpy\text{-}COOH)(PF_6)_2$	3.65 ± 0.56	520 ± 1.5	525 ± 7	0.495 ± 0.061	5.57 ± 0.13	4×10^4
$Ru(dmb)_2(bpy\text{-}(CH_2)_3COOH)(PF_6)_2$	1.70 ± 0.23	486 ± 13	545 ± 6	0.263 ± 0.120	6.09 ± 0.03	2×10^4
$Ru(dmb)_2(bpy\text{-}acac)(PF_6)_2$	2.02 ± 0.14	487 ± 12	535 ± 18	0.292 ± 0.148	4.33 ± 0.32	9×10^3

[a] I_{sc} is the short circuit photocurrent and V_{oc} is the open circuit photovoltage for four samples of each dye in 0.5M NaI/0.05M I_2 propylene carbonate electrolyte excited with 350 mW of "white light". The error is ± 1σ and more details are in the Experimental Section. [b] V_{oc} ± 1σ for three samples of each dye in 0.1 M TBAH propylene carbonate electrolyte. [c] IPCE ± 1σ for seven samples of each dye in 0.5 M NaI/0.05 M I_2 propylene carbonate electrolyte. [d] Surface coverage for samples in foonotes *b* and *c* measured by absorbance spectroscopy. [e] Adduct formation constants measured spectroscopically as described in the text.

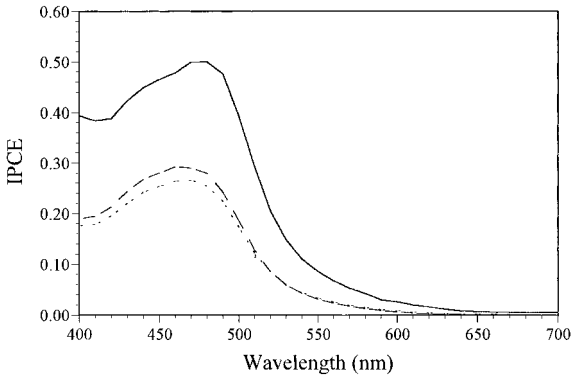

Figure 4. The photoaction spectra of the sensitizers bound to TiO_2 in a regenerative solar cell: (—) is $Ru(dmb)_2(bpy\text{-}COOH)(PF_6)_2$; (- -) $Ru(dmb)_2(bpy\text{-}(CH_2)_3COOH)(PF_6)_2$; (— —) $Ru(dmb)_2(bpy\text{-}acac)(PF_6)_2$. IPCE is the incident-photon-to-current efficiency. An average of seven samples are shown. The electrolyte consists of 0.5 M NaI/0.05 M I_2 in propylene carbonate.

photocurrent to decrease to 85% of the initial value was found to be 25 ± 1 min for $Ru(dmb)_2(bpy\text{-}acac)^{2+}/TiO_2$, 75 ± 5 min for $Ru(dmb)_2(bpy\text{-}(CH_2)_3COOH)^{2+}/TiO_2$, and 75 ± 5 min for $Ru(dmb)_2(bpy\text{-}COOH)^{2+}/TiO_2$. Experiments were also performed on a longer time scale. After 15 h of irradiation the photocurrent dropped to 65, 64, and 57% of the initial values for $Ru(dmb)_2(bpy\text{-}COOH)^{2+}/TiO_2$, $Ru(dmb)_2(bpy\text{-}(CH_2)_3COOH)^{2+}/TiO_2$, and $Ru(dmb)_2(bpy\text{-}acac)^{2+}/TiO_2$, respectively. These times reflect the general stability observed in many photoelectrochemical and spectroscopic experiments: $Ru(dmb)_2(bpy\text{-}COOH)^{2+}/TiO_2 \sim Ru(dmb)_2(bpy\text{-}(CH_2)_3COOH)^{2+}/TiO_2 > Ru(dmb)_2(bpy\text{-}acac)^{2+}/TiO_2$.

Surface attachment to transparent nanostructured TiO_2 and ZrO_2 films allowed excited state absorption measurements to be performed in a transmission mode. Shown in Figure 5 are the excited state absorption difference spectra of the three sensitizers bound to ZrO_2 films in 0.1 M $LiClO_4$ propylene carbonate electrolyte after excitation with a pulse of 532 nm light. The difference spectra are typical of Ru(II) polypyridyl excited states in fluid solution, and isobestic points are clearly observed. Unlike fluid solution, the kinetics on the ZrO_2 surface become complex and require two exponentials for fitting. Alternatively the kinetics are well described by the Kohlrausch−Williams−Watts (KWW) function,[19] eq I. A mean lifetime, $\langle\tau\rangle$, or a mean rate constant $\langle k\rangle$ was calculated with eq II where

$$\Delta A(t) = \alpha \exp\left(-\frac{t}{\tau}\right)^{\beta} \qquad 0 < \beta < 1 \tag{I}$$

$$\frac{1}{\langle k\rangle} = \langle\tau\rangle = \left(\frac{\tau}{\beta}\right)\Gamma\left(\frac{1}{\beta}\right) \tag{II}$$

Γ represents the gamma function. Mean lifetimes are 520 ns for $Ru(dmb)_2(bpy\text{-}COOH)^{2+}/ZrO_2$, 380 ns for $Ru(dmb)_2(bpy\text{-}(CH_2)_3COOH)^{2+}/ZrO_2$, and 690 ns for $Ru(dmb)_2(bpy\text{-}acac)^{2+}/ZrO_2$, under these conditions. The excited state absorbance difference spectra of the sensitizers anchored to TiO_2 display only a broad absorption bleach through the visible region. Shown in Figure 6 are kinetic traces observed at the isobestic point in 0.1 M $LiClO_4$ propylene carbonate. On a longer time scale these transients cleanly return to the baseline. If one assumes that the isobestic point is the same for ZrO_2 and TiO_2, then the kinetics observed at this wavelength can be assigned to the formation and loss of the oxidized sensitizer without possible complications from unquenched MLCT excited states. No rise time was observed for this transient under any conditions. The kinetics shown in Figure 6 are complex but well described by the KWW model. Mean rate constants for three representative samples are summarized in Table 4.

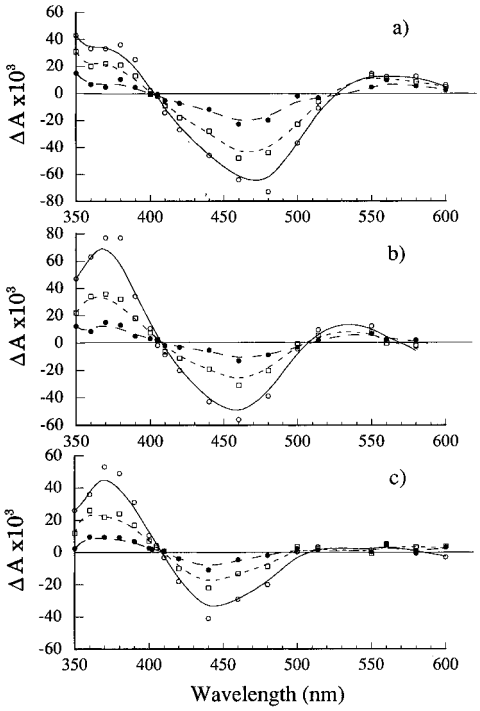

Figure 5. Excited state absorption spectra of the sensitizers bound to transparent sol−gel processed ZrO_2 films in 0.1 M $LiClO_4$ propylene carbonate: (a) $Ru(dmb)_2(bpy\text{-}COOH)^{2+}/ZrO_2$; (b) $Ru(dmb)_2(bpy\text{-}acac)^{2+}/ZrO_2$; (c) $Ru(dmb)_2(bpy\text{-}(CH_2)_3COOH)^{2+}/ZrO_2$. The samples were excited with 532 nm light (8 ns, 10 mJ/pulse) and the spectra are shown 30 ns, 200 ns, and 1 μs after the laser pulse.

Discussion

New sensitizers were successfully prepared and utilized in regenerative solar cells. The bpy-acac derivative was designed to take advantage of the chelate effect and yield more robust sensitizer-to-surface linkages. However, photocurrent stability studies consistently show a higher degree of degradation than those sensitizers bound through a carboxylic acid group. While photocurrent stability may reflect other factors, the measured adduct formation constants are also indicative of a less stable surface linkage. Adduct formation constants in the range of

(19) (a) Kohlrausch, R. *Annalen* **1847**, *5*, 430. (b) Williams, G.; Watts, D. C. *Trans. Faraday Soc.* **1971**, *66*, 80.

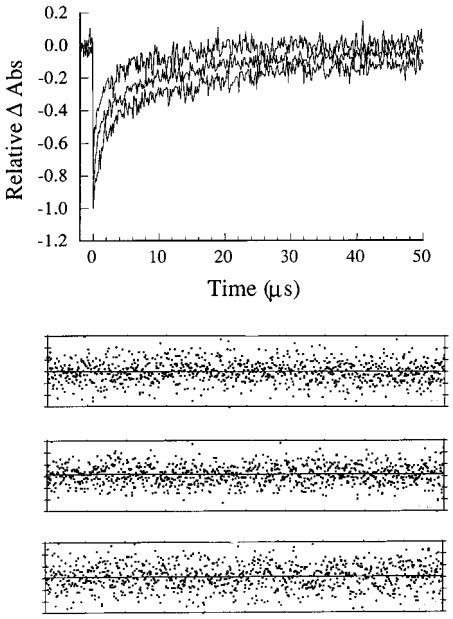

Figure 6. Absorbance change after excitation with a 532 nm light pulse (8 ns, 10 mJ/pulse) for sensitizers bound to nanocrystalline TiO_2 films in 0.1 M $LiClO_4$ propylene carbonate. The upper kinetic trace corresponds to $Ru(dmb)_2(bpy\text{-}COOH)(PF_6)_2$ measured at 402 nm, the middle trace corresponds to $Ru(dmb)_2(bpy\text{-}acac)(PF_6)_2$ measured at 405 nm, and the lower kinetic trace corresponds to $Ru(dmb)_2(bpy\text{-}(CH_2)_3\text{-}COOH)(PF_6)_2$ measured at 405 nm. The kinetics represent an average of 10 laser pulses. The corresponding residuals are shown to demonstrate the goodness of fit to the KWW model.

Table 4. Recombination Kinetics of Sensitizers Anchored to TiO_2[a]

sensitizer	λ_{obs}[b] (nm)	τ[c] (μs)	β[c]	$\langle k \rangle \times 10^4$[d] ($s^{-1}$)
$Ru(dmb)_2(bpy\text{-}COOH)(PF_6)_2$	402	0.38 ± 0.11	0.27 ± 0.03	31.0 ± 2.5
$Ru(dmb)_2(bpy\text{-}(CH_2)_3COOH)(PF_6)_2$	405	1.42 ± 0.22	0.30 ± 0.03	7.41 ± 0.87
$Ru(dmb)_2(bpy\text{-}acac)(PF_6)_2$	405	0.94 ± 0.10	0.29 ± 0.01	9.62 ± 0.77

[a] Kinetics for the recombination of the electron in TiO_2 with the oxidized form of the sensitizer. [b] The wavelength at which the kinetics were observed. [c] Fits to the KWW function, eq I in the text. The error represents one standard deviation for three samples. [d] Mean rate calculated with eq II.

$(2-10) \times 10^4$ M^{-1} for Ru(II) sensitizers based on the 4,4′-$(COOH)_2$-2,2′-bipyridine ligand bound to TiO_2 have been reported in the literature.[6,7b,9] These values are in good agreement with the data reported here for sensitizers which only contain one carboxylic acid group. The adduct formation constant measured for the $Ru(dmb)_2(bpy\text{-}acac)^{2+}$ is similar to that reported for monodentate and bidendate benzene derivatives with oxygen donors bound to TiO_2, $(2-80) \times 10^3$ M^{-1}.[20]

We were somewhat surprised to find quasi-reversible $Ru^{III/II}$ redox chemistry for the surface-anchored sensitizers. The redox chemistry is termed quasi-reversible since the oxidation and reduction current are the same and the peak-to-peak splitting is large. At a minimum this finding provides a new tool for investigating these materials and a means for estimating the energetics of surface-bound sensitizers. In addition, it may lead to some insight into questions regarding surface or bulk carrier transport through the porous nanocrystalline TiO_2 network.[21] A likely explanation for this voltammetry stems from the fact that the colloidal TiO_2 film does not completely cover the SnO_2 substrate.[22] A fraction of the sensitizers, $< \sim 10^{-10}$ mol/cm^2, could bind to SnO_2 where they can be reversibly oxidized electrochemically.[9a] However, the surface coverage measured by voltammetry is much higher, and in the absence of an obvious electron mediator, self-exchange electron transfer processes across the nanocrystalline TiO_2 surface(s) could account for the high electroactive surface coverage. We note that the surface coverages measured spectroscopically are consistently at least an order of magnitude greater than those measured electrochemically, which indicates that > 90% of the sensitizers in the porous TiO_2 film are not electrochemically accessible on this time scale.

Interfacial electron transfer rate from TiO_2 to the oxidized sensitizer is significantly faster for $Ru(dmb)_2(bpy\text{-}COOH)^{2+}/TiO_2$ than for the other two sensitizers. It has recently been shown that the dynamics of this process can be directly related to open circuit photovoltages, V_{oc}, in regenerative solar cells based on these materials.[23] Qualitatively, the open circuit photovoltages measured in the absence of iodide do track the observed kinetics. While the differences in V_{oc} are relatively small, these results do demonstrate how molecular level design can be used to tune interfacial electron transfer dynamics.

A remarkable result from these studies is the observation of efficient light-to-electrical energy conversion from sensitizers which possess a *n*-propyl chain between the chromophore and the surface link. It has previously been thought that intimate electronic coupling between the sensitizer and the chromophore is required for efficient photocurrent production.[24] If corrections are made for the fraction of light absorbed then the photocurrent efficiencies for $Ru(dmb)_2(bpy\text{-}acac)^{2+}/TiO_2$ and $Ru(dmb)_2(bpy\text{-}COOH)^{2+}/TiO_2$ are within experimental error the same. Further, the lack of a measurable rise time for the formation of Ru(III) indicates that the electron injection rates is $>5 \times 10^7$ s^{-1} for all three surface-bound sensitizers. Since the *n*-propyl spacer is not rigid the chromophoric unit may be at similar distances from the surface for all three sensitizers. However, the equivalent corrected IPCE for $Ru(dmb)_2(bpy\text{-}acac)^{2+}/TiO_2$ and $Ru(dmb)_2(bpy\text{-}COOH)^{2+}/TiO_2$ indicates that intimate electronic coupling between the chromophoric ligand and the surface link is not a strict requirement in the design of sensitizers for photovoltaic applications.

Conclusion

The preparation of a new Ru(II) polypyridyl sensitizer with a pendant acetylacetonate derivative has been achieved. The sensitizer binds to porous nanocrystalline TiO_2 films with surface coverages slightly lower than related sensitizers based on carboxylic acid groups. When employed as photoanodes in regenerative solar cells, the sensitizer efficiently converts photons to electrons with monochromatic efficiencies ≥ 0.30. Since the surface link and the sensitizer are separated by a *n*-propyl spacer, the high efficiency indicates that intimate electronic contact between the surface link and the chromophoric ligand is not a strict requirement in the design of sensitizers for photovoltaic devices.

Acknowledgment. We would like to thank the National Renewable Energy Laboratory Grant NREL XAD-3-12113-04) and the National Science Foundation (Grants CHE-9322559 and CHE-9402935) for support of this research. T.A.H. acknowledges financial support from a Sonneborne Fellowship.

IC960419J

(20) Moser, J.; Punchihewa, S.; Infelta, P.; Gratzel, M. *Langmuir* **1991**, *7*, 3012.
(21) Sodergren, S.; Hagfeldt, A.; Olsson, J.; Lindquist, S.-E. *J. Phys. Chem.* **1992**, *96*, 5983.
(22) Cao, F.; Oskam, G.; Searson, P. C.; Stipkala, J. M.; Heimer, T. A.; Farzad, F.; Meyer, G. J. *J. Phys. Chem.* **1995**, *99*, 11974.
(23) Argazzi, R.; Bignozzi, C. A.; Heimer, T. A.; Castellano, F. N.; Meyer, G. J. *J. Am. Chem. Soc.* **1995**, *117*, 11815.
(24) Fujihira, M.; Ohnishi, N.; Osa, T. *Nature* **1977**, *268*, 226.